Supporting Information

Untangling surface oxygen exchange effects in $YBa_2Cu_3O_{6+x}$ thin films by electrical conductivity relaxation

P. Cayado[a], C. F. Sánchez-Valdés[a], A. Stangl[a], M. Coll[a], P. Roura[b], A. Palau[a], T. Puig[a] and Xavier Obradors[a,*]

Figure S1). The influence of the gas flow on the oxygen diffusion kinetics for the out–diffusion process. Figure a) shows the evolution of the oxygen exchange relaxation time (?) for the out diffusion process with the gas flow at different temperatures. It is observed that ? reduces at any temperature as the gas flow increases. Figure b) demonstrates that, as the gas flow increases, the differences in ? for different temperatures are reduced so approaching to the equilibrium state. Therefore, it is important to carry out the experiments at high gas flows to maintain the boundary layer in equilibrium with the ambient and avoid local changes in the oxygen partial pressure that can modify locally the diffusion processes.

Figure S2). Superconducting properties (T_c and J_c(T)) determined for inductive magnetic measurements. Figure a) shows the temperature dependence of normalized magnetization measured after a zero field cooling process at low external magnetic fields (H = 1- 5 Oe) of three films with different degrees of oxygen content. The processes followed to achieve such oxygen contents are indicated in the figure caption. The c-axis lattice parameter of the two samples having the highest and lowest oxygen content was determined: c=1.17499 (8) nm and c=1.16980 (6) nm, respectively. The T_c values and c-axis parameters are consistent with previous determinations of the relationship between these two parameters in $YBa_2Cu_3O_{6+x}$. Figure b) shows how the oxygen content directly influences the critical current density J_c(T) of YBCO films. It's seen that a decrease of T_c directly leads to a J_c reduction while when T_c is already very close to optimal still strong modifications of J_c(T) can occur. The film with the longest oxygen annealing treatments displays structural and superconducting properties of a fully oxygenated sample.

Figure S3). TEM cross section images of a typical YBCO film grown by CSD. a) Low resolution TEM image of a YBCO film grown on a LaAlO3 single crystalline substrate where it's appreciated that a low porosity is displayed. b) High resolution TEM image with a detail of the interface of the epitaxial YBCO film and the substrate where the high quality of the epitaxy is appreciated. A detailed analysis of the microstructure of these films has been previously presented in ref. 90 of the manuscript.

Figure S4). SEM images of a YBCO film with a silver coating and corresponding EDX analysis of a typical microparticle observed in the image. A uniform coating of 100 nm Ag was achieved by sputtering, however, after thermal annealing at 300 °C for about 5 h the Ag films has been transformed to a discontinuous coating of micro/nanoparticles. Figure a) shows the Ag micro and nanoparticles formed after annealing the Ag coated film at 500 ºC for about 5 h. Figures b) and c) show EDX measurements of a selected microparticle which confirms the composition as Ag.

References

S1. J. Gázquez, M. Coll, N. Romà, F. Sandiumenge, T. Puig and X. Obradors*, Supercond. Sci. Technol.* 25, 65009 (2012).

S2. X. Obradors, T. Puig, S. Ricart, M. Coll, J. Gázquez, A. Palau and X. Granados*, Supercond. Sci. Technol.* 25, 123001 (2012).

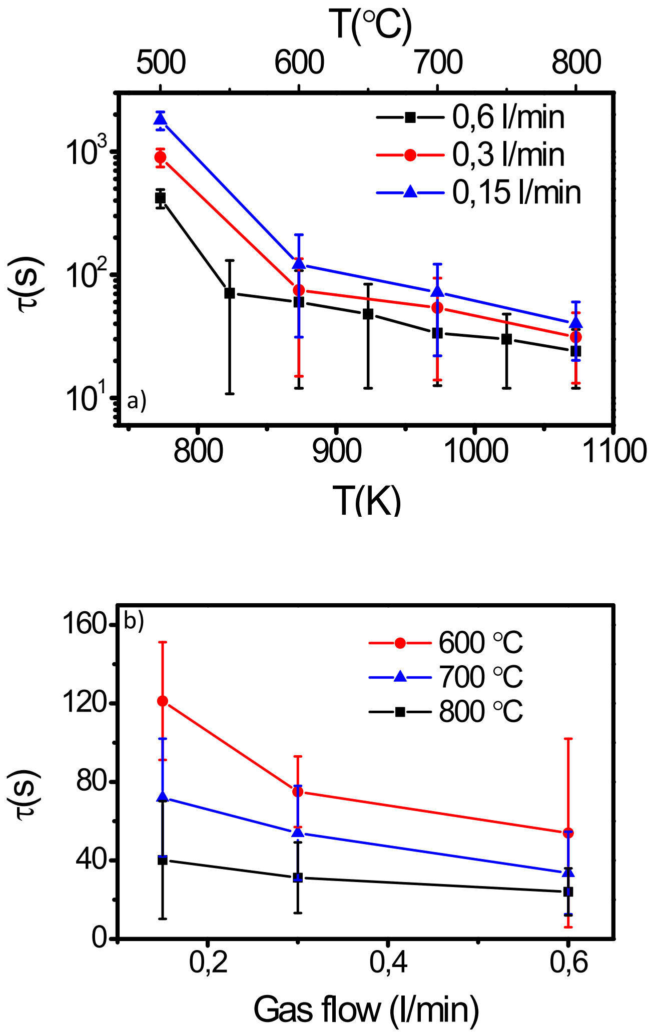

Figure S1. Evolution of the diffusion relaxation time (τ) with a) the temperature for different gas flow values and b) the gas flow for different temperatures.

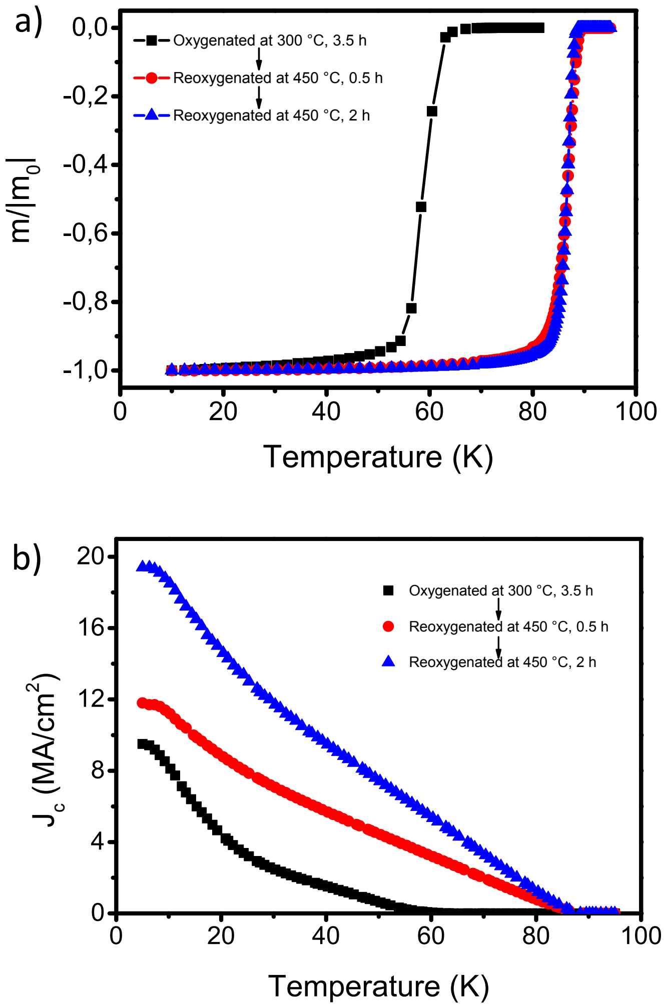

Figure S2. Influence of oxygenation degree on the superconducting properties T_c and $J_c(T)$. Three YBCO films samples are reported having different degrees of oxygen content. (black squares) corresponds to a YBCO films oxygenated at 300ºC during 12.600 s (3,5 h); (red circles) the YBCO film oxygenated at 300 ºC is further oxygenated during 1.800 s at 450ºC; (blue triangles) the YBCO film oxygenated at 300ºC is further oxygenated during 7.200 s at 450ºC. a) Temperature dependence of low field (H= 1-5 Oe) magnetization measurements after a zero field cooling process allowing to determine T_c; b) Temperature dependence of the self-field critical current density $J_c(T)$ in the three films referred above.

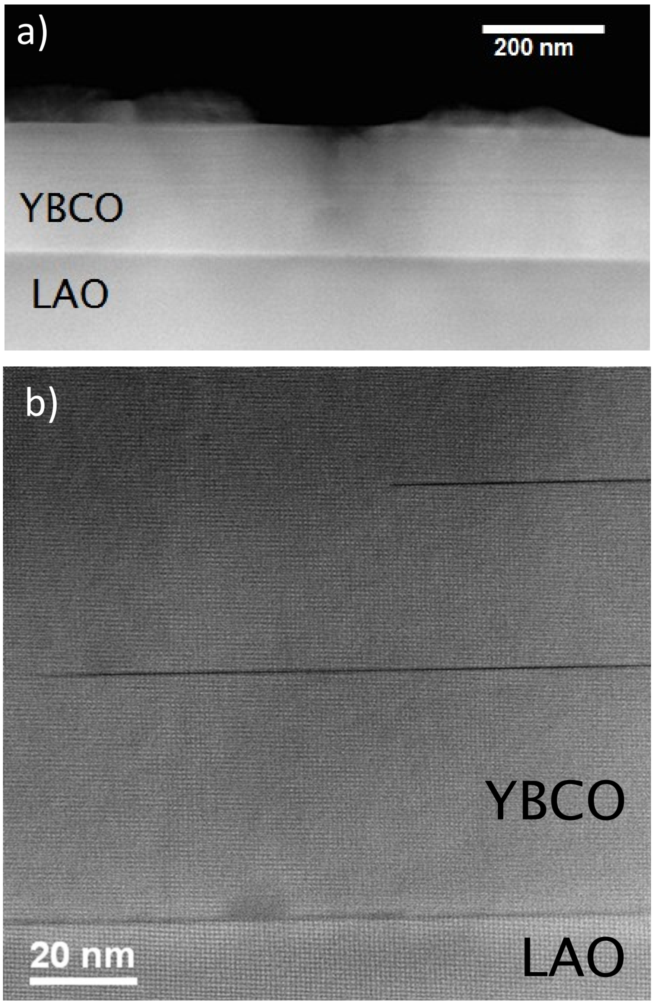

Figure S3). a) Typical low resolution cross section TEM image of a YBCO film grown on $LaAlO_3$ single crystals by the CSD approach where it's appreciated that the films have a high density and low porosity. b) High resolution TEM image of the epitaxial YBCO film grown on a $LaAlO_3$ substrate. See refs. S1 and S2.

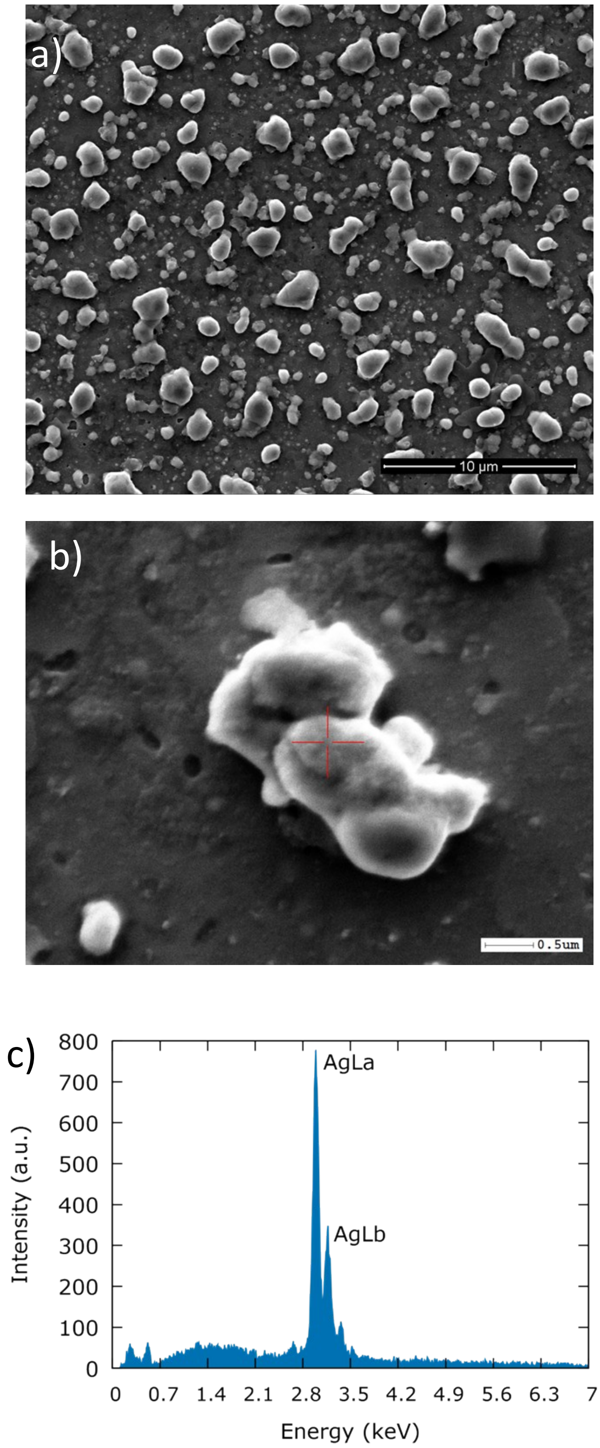

Figure S4. a) SEM image of a YBCO film with a silver coating after annealing at 500 °C. b) Detail of an Ag microparticle where EDX analysis has been carried out. c) EDX analysis of the microparticle observed in b).